[Article ID] 1003- 6326(2001)03- 0387- 04

# Microstructures and properties of tungsten inert gas welding joint of super-eutectic ZA alloy

LIU Xiurzhong(刘秀中)<sup>1</sup>, DONG Borling(董博玲)<sup>1</sup>, ZHAO Dong-jian(赵东建)<sup>1</sup>, ZHU Xing-hai(朱兴海)<sup>2</sup> (1. School of Materials Science and Engineering, Shandong University, Ji nan 250061, P. R. China;

2. Jinan Research and Inspect Institute of Boiler and Pressure Container, Ji nan P. R. China)

[Abstract] The microstructure of butt-welding joint of supper-eutectic ZA alloy in TIG welding was analyzed through optical microscope and transmission electronic microscope. The results show that the weld seam microstructure is fine and mainly composed of columnar crystals and minor equiaxed crystals, the microstructure in the zone near the weld seam is coarse columnar crystals, and the grain in heat-affected zone does not grow markedly. The joint microstructure at room temperature is consisted of  $\beta$  phase (rich Al),  $\Re$ Zn,  $\varepsilon$  phase (CuZn compound), Al<sub>4</sub>Cu<sub>9</sub> and other compounds. The hardness of the weld bond area and the tensile strength of the joint are a little higher than that of base materials. The specific elongation of the weld and bond area is a little lower than those of base materials.

[Key words] ZA alloy; welding joint; microstructure; properties

[CLC number] TG 113

[Document code] A

#### 1 INTRODUCTION

Super-eutectic ZA alloy is a new type of material that is studied, developed and most widely used in mould engineering. Because both the melting point of the alloy and boiling point of Zn are low, while the temperature of fusion welding heat source is high, great change in microstructure and property of the butt-welding joint is expected to take place. It is only the braze welding and acetylene welding technology that are introduced in China, while the study on tungsten inert gas(TIG) technology is little. There is almost no study concerning the microstructures and properties of the welding joint of super-eutectic ZA alloy processed by TIG welding so far<sup>[1~5]</sup>.

In this paper, the microstructures and characteristics of the welding joint of super-eutectic ZA alloy processed by TIG welding are investigated by optical microscopy and transmission electron microscopy (TEM) on the basis of the previous research on the welding technology of ZA alloy, and the properties of the welding joint are tested and analyzed. The results in this paper provide a basis for the further study of welding behavior of the alloy.

#### 2 EXPERIMENTAL

The base material used in the experiment is a new type of super-eutectic ZA alloy. The plate with size of 6 mm × 100 mm × 120 mm was prepared by metal mould casting. The chemical composition and

mechanical properties of the base material are listed in Table 1 and Table 2. The same super-eutectic ZA alloy was used as filler material, which was metal mould cast into welding rod with a diameter of 4 mm and a length of 300 mm. The self-made special welding flux was used in this experiment.

W (Al)W (Cu)W (Mn)W (Mg)W (Zn)8~ 10 $3\sim 5$  $0.2\sim 0.5$  $0.02\sim 0.05$ Balanced

 Table 2
 M echanical properties of base material

 Tensile strength,  $σ_b/MPa$  Specific elongation,  $δ_5/%$  

 ≥300
 >  $3 \sim 4$ 

A WSE-315 type of manual tungsten inert gas arc welder were used. The welding structure is in the form of butt, and the groove is asymmetric X type. The sample was first cleaned, then clipped on the special jig. After the specimen was preheated to 100 ~ 120 °C by oxide acetylene flame, the welding rod and the specimen were coated with the welding flux, then the specimen was welded according to the adjusted process parameters illustrated in Table 3.

The leftward welding method was used. A backing was put under the specimen to be welded. The welding rod was inclined with an angle of 40°~ 50°. In order to fill up the arc hole and to avoid collapse, the weld rod should be moved in a circulars way as the welding process completed. After the welding

① [Foundation item] Project (993175101) supported by the Science and Technology Development Program of Shandong Province [Received date] 2000- 07- 02; [Accepted date] 2000- 10- 08

**Table 3** Process parameters of TIG welding

Welding current/ A	Diameter of tungsten electrode/ mm	Flow rate of argon /(L•min <sup>-1</sup> )	Current type
60~ 80	3. 2	6~ 7	Alternating current

finished, the weld seam was firstly examined to see whether there exist gas cavity, inclusions, crack and unwelded bond zone on the surface. Finally the microstructures of the welding joint were examined and the properties of the welding joint were tested.

## 3 RESULTS AND DISCUSSION

### 3. 1 Microstructures of welding joint

The welding joint may be classified into seam, weld bond zone, heat-affected zone and the matrix according to the microstructure characteristics of the TIG welding joint of the super-eutectic ZA alloy, the microstructures corresponding to various zones are illustrated in Fig. 1.

From the chemical composition, Zm-Al binary diagram [3] and isothermal phase diagram of Zm-Al-Cu (as shown in Fig. 2), it can be seen that the base material is composed of primary  $\beta$ , binary eutectic ( $\beta$ +  $\eta$ ) and ternary eutectic ( $\beta$ +  $\eta$ +  $\epsilon$ ) phases. Some fine compound particles distribute on the eutectic matrix. The primary  $\beta$  phase is massive and the white blocky massive phase is  $\epsilon$  phase. The microstructure

indicated by white spot  $\mathcal{E}$  phase distributing on the deep color matrix is ternary eutectic ( $\beta$ +  $\eta$ +  $\mathcal{E}$ ) phase  $^{[6\sim 8]}$  and this phase is mainly columnar crystal with coarser crystal grain. The microstructure of the joint interface is mainly composed of fine dendrite and a small amount of columnar crystal. The columnar crystal and chrysanthemum type crystal are binary eutectic ( $\beta$ +  $\eta$ ) phase and primary  $\beta$  phase. The phase of the dendrite branch is primary  $\beta$ . The TEM images of the  $\beta$ ,  $\eta$ ,  $\mathcal{E}$  phases and corresponding selected area electron diffraction (SAD) patterns are showed in Fig. 3. It can be seen that there exist some fine polygonal sub-grains in  $\eta$ -Zn grain. There are some dislocation loops in  $\beta$  (rich Al) grain.

The cooling rate of welding is higher than that of casting. The melt in the molten bath crystallizes fast which make crystal to be fine and to form columnar dendrite, therefore the weld seam is mainly composed of columnar crystals. But a remarkable change on the microstructures takes place in the weld bond zone. There exist coarse dendrites and larger amount of eutectic crystals near the seam. This is because the zone is in partly molten state, and some eutectic crystals with low melting point may melt firstly; while the weld bond zone cool fast than other zones and there is not enough time for a part of primary β phase to precipitate, then the eutectic transformation takes place. The microstructures in the heat-affected zone tends to be fine. The reason is that the melting point of the super-eutectic ZA alloy is low and the coefficients of

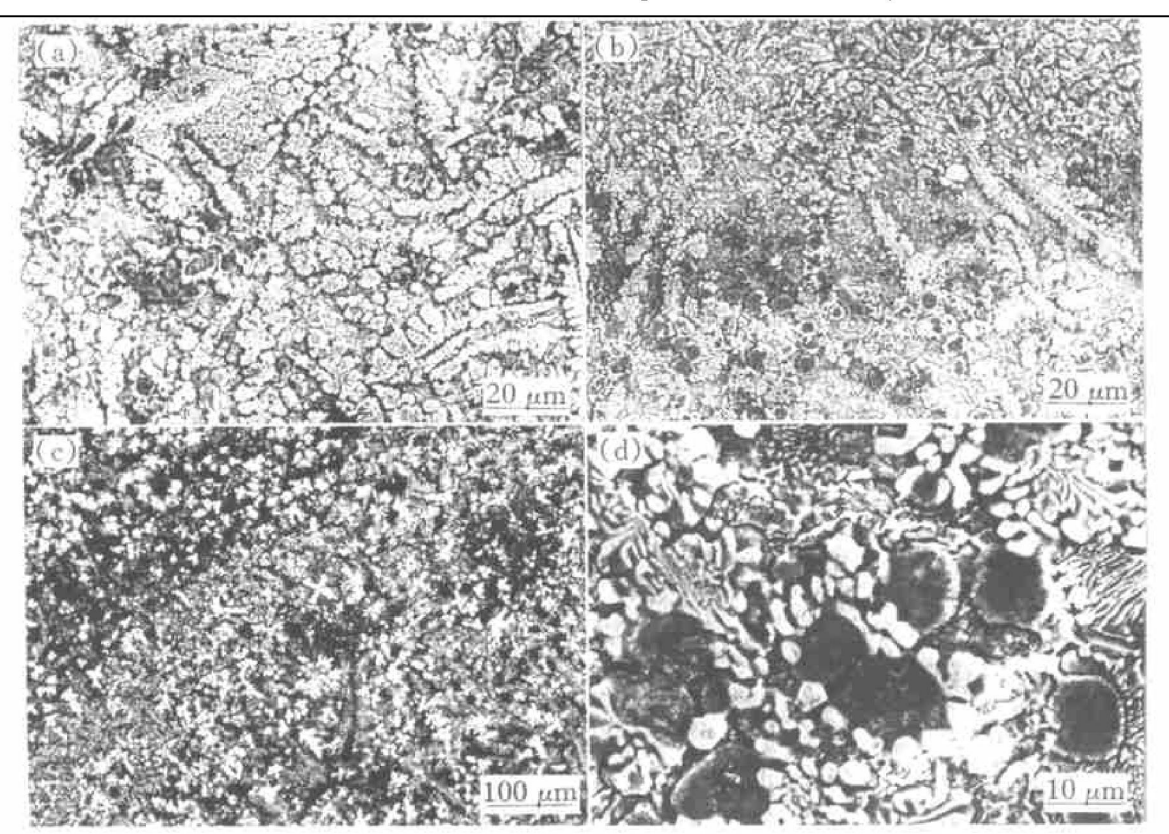
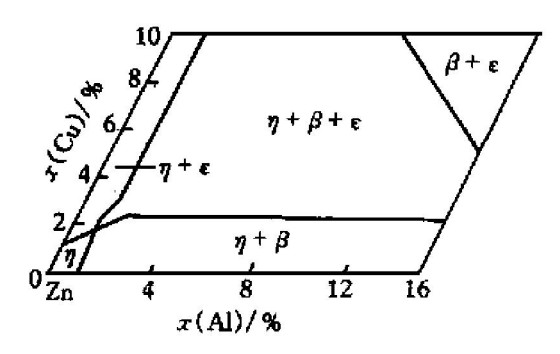


Fig. 1 Microstructures of welding joint
(a) —Joint interface; (b) —Weld bond zone; (c) —Heat-affected zone; (d) —Base material

Base

material



**Fig. 2** Isothermal phase diagram of Zm-A+Cu alloy at 300 °C

heat transmission is large. Although the maximum temperature of the heat cycle is very high, the retention period was short. Therefore the grain in the heat-affected zone recrystallizes to fine microstructure.

## 3. 2 Properties of welding joint

The tensile experiment results of the welding joint are listed in Table 4. Table 4 shows that the tensile strength of the welding joint is higher than that of the base material, but the specific elongation of the welding joint is a little lower than that of the base material. Most of the fracture position is in the base material. The welding joint is more compact than base material and the crystal grain of the welding joint is fine. This makes the properties increase. In the heat-affected zone the recrystallization takes place and the microstructures tend to be fine, so the

Table 4	M echanical p	roperties of	welding joint
Sample number	Tensile strength/ MPa	Eelongation /%	Fracture position
1	350	3.5	Base material
2	360	3. 2	Base material
3	362	3.0	Base material

4.0

341

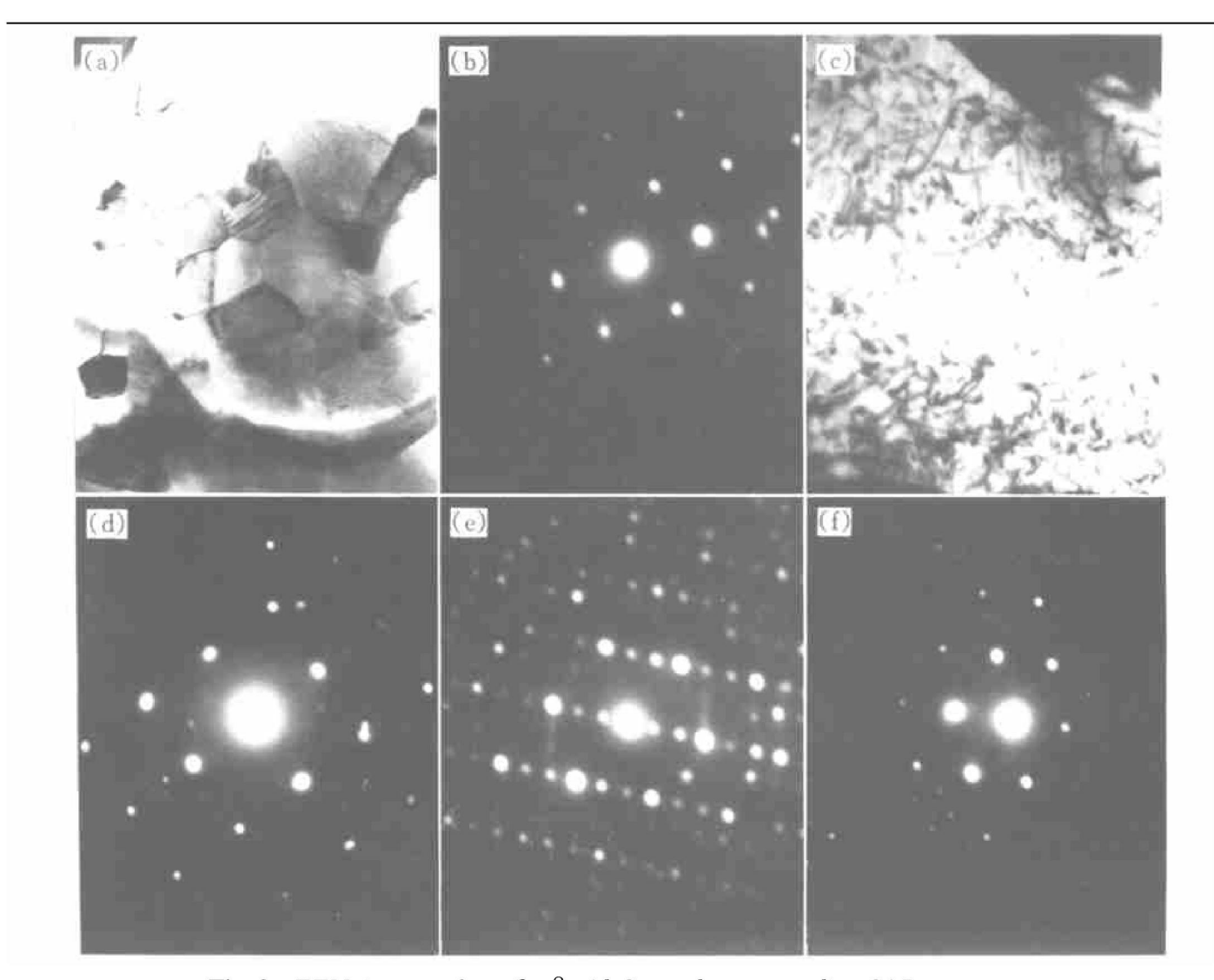


Fig. 3 TEM images of ε, η, β, Al<sub>4</sub>Cu<sub>9</sub> and corresponding SAD patterns
(a) —Polygonal sub particles in granular η grain; (b) —Corresponding SAD pattern of η phase;
(c) —Dislocations and dislocation loops in β grain; (d) —Corresponding SAD pattern of β phase;

(e) —SAD pattern of ε phase; (f) —SAD pattern of Al<sub>4</sub>Cu<sub>9</sub>

properties of the heat-affected zone do not decrease. In addition, the evaporation of Zn during the welding process makes Zn content near the weld seam and the weld bond zone decrease, while the content of other elements such as Al, Cu, Mn increase. The increase of the alloy element content strengthens the material which results in the tensile strength increasing, but the plasticity and toughness decreasing. The property reaches an optimum value when the content of Al is  $4\% \sim 5\%$ . As the content of Al increases, the strength may further increase, but the plasticity and the toughness decrease a little [9, 10].

The hardnesses of the welding joint are listed in Table 5.

 Table 5
 Brinell hardness of welding joint

Sample number	Weld seam	Weld bond zone	Base material
1	132	122	124
2	130	127	120
3	129	124	119
Average	130	124. 33	121

It is found from Table 5 that the hardness of the welding seam and weld bond zone is higher than that of the base material. The Brinell hardness of the welding seam is highest and is up to 130. The hardness of the weld bond zone is lower than that of the weld seam and it is only a little higher than that of the base material. During the welding process, the welding electric arc imposes intense stirring on the molten bath, the gas and inclusions in the weld molten bath can be discharged under suitable welding parameters, which reduces and avoids defects at joint interface. In addition, the cooling rate is large during welding and there is a large supercooling as the material in the molten bath crystallizes, so the microstructure is fine. Zn and other alloy element contents are different in the weld seam and molten bath due to the evaporation of Zn during the welding process. The content of Zn is lower in the weld seam than that in the weld bond zone, while the contents of the Al and Cu are higher than that in the weld bond zone. Both Al and Cu can increase the hardness of Zn, especially  $Cu^{[1, 7, 8]}$ 

## 4 CONCLUSIONS

1) The super-eutectic ZA alloy is welded by TIG process using special weld rod. The microstructure of welding seam is fine and is mainly composed of fine

dendrite and a small amount of columnar crystals. The microstructure in the molten zone changes markedly, the zone near the welding seam is coarse columnar crystal. The grain in the heat-affected zone does not become coarsen because of recrystallization.

- 2) The tensile strength of the welding joint of the super-eutectic ZA alloy processed by TIG is not lower than that of the base material. The specific elongation is similar to or a little lower than the base material. The hardness of the weld seam and weld bond zone is higher than that of the base material and the hardness reaches a maximum in the weld seam.
- 3) There exist some polygonal sub-particles in  $\mathfrak{P}$  Zn grain at the welding seam, this makes the grain fine and intensify the tensile strength.

## [ REFERENCES]

- Nuttall K. The damping characteristic of a superplastic Zn-Al eutectoid alloy [J]. Journal of the Institute of Metals, 1971, 99: 266-270.
- [2] GU Ming-yuan, CHEN zheng-yang, WANG Zhang-min, et al. Damping characteristic of Zrr Al matrix composites [J]. Script Metallurgical et Material, 1994, 30 (10): 1321-1326.
- [3] Sahoo M, Whiting L V. Foundry characteristics of sand cast Zrr Al alloys [J]. AFS Transactions, 1984, 38: 861 – 870.
- [4] CHENG Trjiu, HAO Yuan. Current status of zinc martrix composites [J]. Materials Review, 2000, 14(3): 29-31.
- [5] CHEN Yurrgui, TU Ming-jing, SHEN Bao luo, et al. Dimensional shrinkage of superaturated ZA27 and influnence of phase transformation [J]. The Chinese Journal of Nonferrous Metals, (in Chinese), 1998, 8(2): 254-258.
- [6] ZHU Y H. Complex microstructural changes in as cast eutectoid Zn Al alloy [J]. Journal of Materials Science, 1994, 29: 1549–1552.
- [7] ZHANG Zhong ming, WANG Jim cheng, XU Dong hui, et al. Damping capacities of supersaturated ZAC27 alloy and its relation with microstructural evolution [J]. Trans Nonferrous Met Soc China, 2000, 10(3): 306–312.
- [8] ZHANG Zhong mong. Phase transformation, properties and damping mechanism of ZnAl alloy [D]. Xi an: Northwestern Polytechnic University, 1999. 81.
- [9] Tagami M, Ohtani T, Usami T. Effects of heat treatment, contents of Cu and Mg, and rolling reduction on the damping capacity and mechanical properties of Zrr 22% Al alloys [J]. Journal of Japan Material Science, 1992, 27: 1212- 1216.
- [10] ZHANG Zhong ming, WANG Jim cheng, XU Donghui, et al. Effect of Al, Cu, Mg content on mir crostructure and damping capacity of zinc based alloy [J]. The Chinese Journal of Nonferrous Metals, (in Chinese), 1999, 9(Suppl. 1): 1-6.

(Edited by YANG Bing)